Speckle Interferometry: A Review of the Principal Methods in Use for Experimental Mechanics Applications

P. Jacquot

Nanophotonics and Metrology Laboratory, Swiss Federal Institute of Technology, CH-1015 Lausanne, Switzerland

ABSTRACT: With its nearly 40 years of existence, speckle interferometry (SI) has become a complete technique, widely used in many branches of experimental mechanics. It is thus a challenging task to try to summarise in a couple of pages its principal characteristics from both theoretical and practical points of view. Admittedly, even though this goal is not met here, it appeared worth attempting to provide the photomechanics community with a discussion of the ins and outs of the technique. The necessity of a vocabulary free of ambiguity was a prerequisite, and hence the first section is a plea for a clearer definition of the discipline. Moreover, this section offers the opportunity to re-examine the basic aspects of SI. Then, the main features of the method are briefly considered following a strengths, weaknesses, opportunities and threats (SWOT) analysis. Endowed with a lot of specific advantages, compared with other whole-field methods, SI can play an increasing role in photomechanics.

KEY WORDS: *deformation analysis, experimental mechanics applications, methodologies, speckle interferometry*

Introduction

The birth of SI dates back at least to the early 1970s, when Leendertz and Butters published their seminal articles [1, 2]. These articles arouse a considerable interest among the holographic interferometry (HI) community. Scientists of this field then realised that the direct recording of a two-beam interference pattern between a reference and a speckle wave carries in itself the phase information of the speckle wave, without the need to reconstruct its 3D complex amplitude as in holography – a step appearing deceptively simple nowadays. A huge amount of scientific literature pertaining to SI, impossible to be all cited here, is currently available, very rich in both theoretical and practical considerations. The few references [3–7], and the references therein, give at least the first bases of the discipline. Referring to the number of recent well-attended international conferences including in their programmes SI techniques as a major topic (as e.g. [8]), the research and application fields are by no means exhausted. Besides such bootstraps, this contribution attempts to analyse the role of SI in experimental mechanics, mainly inspired by the papers [9–11]. For this purpose, it seemed convenient to borrow an approach usually employed in a business context, i.e. the strengths, weaknesses, opportunities and threats (SWOT) analysis.

A serious difficulty accompanying any treatment of SI lies in the absence of a clear and agreed upon definition of the discipline. On the contrary, many designations can be found, not exempt of possible confusions. Examples of these designations are, besides the old terminology 'ESPI', for electronic speckle-pattern interferometry, electro-optic interferometry, TV holography, digital speckle interferometry, etc., with many adjunctions such as in-line, shearing or phase-shifting SI, and so on. 'Digital holography' (DH) is usually free of misinterpretation, but when an expression like 'image-plane digital holography' is encountered, it becomes difficult to perceive the distinction between HI and SI. And what to say about lensless SI? This is why the paper starts with a series of comments about the SI jargon, suggesting at the same time a classification of the questions of general interest.

Being an established technique, SI can be practised using turnkey systems or self-made set-ups, offered on the vast quality equipments and components market. Deliberately, technical considerations about

sources, lenses, cameras, acquisition and processing tools, etc., though of primary importance for a sound and correct operation of the technique, are not treated in order not to overload the manuscript. Let us simply mention that the Internet sites of the many providers are easy to access and well documented.

Glossary and Categorisation

In interferometry, a highly discriminating feature is the state of smoothness of the interfering waves. Smooth waves, similar to plane or spherical waves, arising from optically polished components, possess nearly constant amplitudes and gently varying phases over large volumes. Speckle waves, reflected or transmitted by rough diffusing surfaces, on the contrary, exhibit rapid amplitude and phase fluctuations. There is no way to make a prediction of the evolution of these waves outside the correlation volume – as small as $3 \times 3 \times 100\ \mu m^3$ for visible wavelengths and usual apertures (cf. Equation 3). Although formally the same two-beam interference formula:

$$I_R = I_1 + I_2 + 2\sqrt{I_1 I_2}|\gamma| \cos\varphi, \qquad (1)$$

is applicable, the appearance and the general properties of the resultant intensity, I_R, are at considerable variance, depending on whether the two waves are smooth or whether at least one is a speckle wave. In Equation (1), I_1 and I_2 are the intensities of the two waves, φ their phase difference, and $|\gamma|$ (taken equal to 1 in the rest of the paper) the normalised module of the cross-correlation of the two amplitudes. The arguments of the functions, specifying the observation point, are omitted for simplicity. Among many others, let us point out just two substantial differences:

(i) the resultant intensity has a speckle appearance and not that of a constituted fringe pattern in a speckle interference;
(ii) smooth wave interferometry is invariant under in-plane displacement of plane mirrors placed in either of the beam paths, whereas, with a speckle wave, the in-plane displacement of the diffuser generally creates a new uncorrelated pattern.

Speckle interference patterns need in any case a kind of further decoding step in order to become a source of useful information. Thus, while 'classical interferometry' (CI) is the unanimously accepted designation for smooth wave interferometry, it could be natural to term 'SI' all types of interferences involving speckle waves. Hence, recording the hologram of a diffusing object – nothing else than the recording of an interference pattern between a smooth 'reference' wave and the object speckle wave – would indeed be an SI process. Holographic interferometry, making possible the concomitant reconstruction and the interferometric comparison of two speckle waves recoded at two different instants for two distinct states of a diffuser too would be a genuine SI experiment. Clearly, though logical, the above definition is against common practice. Holography and HI happened before SI [12]. Many treatises on holography and HI, perhaps wrongly, do not pay much attention to the speckle phenomenon. Another strong reason for not including holography and HI in the bosom of SI is the distinctive feature attached to all forms of holography, namely the full 3D reconstruction of the recorded wave – a step absent in SI. This last point will be useful later to distinguish DH from SI techniques. In particular, all the very important discussions in HI about the 3D loci of fringe localisation and the 3D search for the best fringe contrast regions [13] have no counterparts in SI. This does not mean, of course, that the transposition into SI of results specifically obtained in HI is forbidden.

At this point, and according to the first descriptions given in Refs [1, 2], SI can be defined as the set of techniques aiming at creating, recording and taking advantage of a two-beam interference pattern involving at least one speckle wave, with the purpose of directly exploiting the 2D phase information contained in the recording. This definition seems operational, as apparently no known optical arrangements of SI are excluded, and no intruders hosted. Obviously, the generic name 'SI' will have to be complemented with appositions in order to account for the many existing variants of the technique, and for the needs of further categorisation.

Speckle interferometry can be looked at from no less than four cardinal points: the statistical, optical, mechanical and processing points of view, each reflecting a particular centre of interest (Figure 1).

Statistical aspects

Statistically, Equation (1) gives rise to several interpretations: the resultant intensity, I_R, obeys different groups of statistical behaviour, depending on whether one smooth and one speckle or two speckle waves interfere. On the usual assumptions leading to Gaussian speckle fields [14], the speckle phase itself is uniformly distributed on a 2π interval. It follows that the interferometric phase φ of Equation (1),

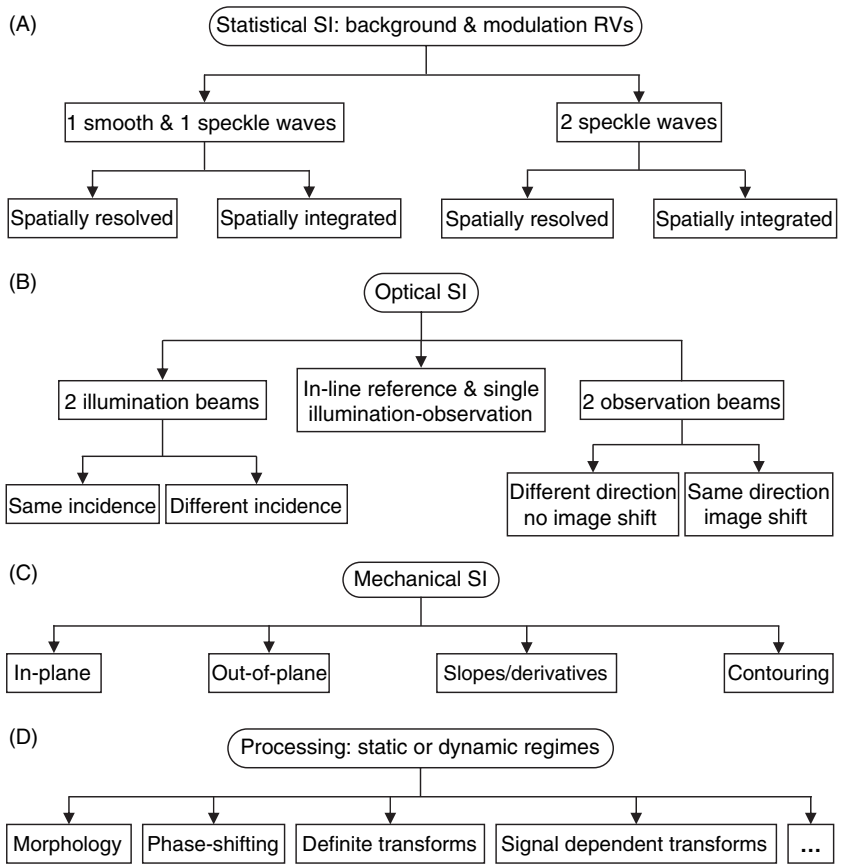

Figure 1: Possible categorisation of SI, according to the underlying principles of the method: the statistical (A), optical (B), mechanical (C) and processing (D) viewpoints

irrespective of its exact probability density, also takes values in a 2π interval, and all possible realisations of I_R oscillate around the background $2B$ with a modulation $\pm 2M$, where B and M are given by:

$$B = \frac{I_1 + I_2}{2}; \quad M = \sqrt{I_1 I_2}; \quad I_R = 2(B + M\cos\varphi). \qquad (2)$$

The background and modulation, which determine the maximum, the minimum and the average of all possible realisations of the signal – just what is needed for a proper recording – are thus the relevant random variables (RVs) of SI. Clearly, these RVs obey four distinct categories of properties, as depicted in Figure 1A, made of the combination of the two types of interference – one smooth and one speckle or two speckle waves – and of the two spatial integration regimes – with or without spatial integration. Fortunately, the eight probability density functions for background and modulation associated with the four categories are known [14–16]. These statistics are not only of fundamental interest but also of very practical significance, because they lead to record in the best possible conditions the interferometric signal, by choosing the intensities of the fields and the lens apertures, which, given the characteristics of the photo-detector, will optimise the modulation. Second-order statistics are also of great interest, because they give, through the autocorrelation functions, the average spatial variation rate of the RVs. Here, the result can be related to the case of a single speckle field, as the coherent addition with a constant field simply adds a bias to the autocorrelation, and the coherent addition with an uncorrelated speckle field of the same strength follows the same constitutive mechanism as that of a single speckle. The autocorrelations of the complex amplitude and intensity of a single speckle field are narrow-peaked functions, nearly vanishing outside a small volume element – the correlation volume – of transversal and longitudinal dimensions, $\langle S_t \rangle$ and $\langle S_l \rangle$ given by:

$$\langle S_t \rangle = \frac{\lambda d}{a}; \quad \langle S_l \rangle = \frac{8\lambda d^2}{a^2} \qquad (3)$$

where λ is the wavelength, and d/a is related to the maximal aperture of the marginal rays creating the speckle, d being either the distance lens – or diffuser – observation plane, and a the lens aperture or the diffuser transversal dimension. The first case corresponds to the usual speckle formation in SI by means of a lens imaging the diffuser onto the photo-

detector, called subjective speckle. Incidentally, the influence of the lens aperture on the dimension of the correlation volume can be noticed in Figure 3, drawn for another purpose. The second case, the so-called objective speckle, rather unusual in SI, corresponds to a lensless speckle formation, from diffraction of the diffuser. As far as the statistical aspects of SI are concerned, 'subjective' and 'objective' do not represent a really meaningful labelling. The correlation dimensions, Equation (3), are as a rule likened to the dimensions of the 'average' speckle grain. Even in these small volumes, the speckle complex amplitude is not constant, but worse, outside, it is not possible to predict the value of the complex amplitude, except that it follows a circular Gaussian distribution – a fundamental and major difficulty of all interferometric methods involving speckle waves.

The question of the spatial integration regimes may have two answers. Initially, SI recordings were made mostly with very high resolution emulsions, the same as in HI, and the aerial speckle fields could be considered as spatially resolved. However, soon, video cameras, and later charge-coupled device and Complementary Metal Oxide Semiconductor (CMOS), became a standard, moving SI techniques towards the low spatial resolution domain. Evident convenience reasons led to this choice, and now, photo-electric recording is an intrinsic part of SI. Consequently, most of the recordings are now performed in a weak integration regime: there are among one to 10 independent cells within a $6 \times 8\ \mu m^2$ pixel, at 514 nm, for the usual f-number apertures between 5.6 and 22 [11, 15]. The strictly resolved regime is almost impossible to realise, requiring apertures as small as one-hundredth of the focal length. On the contrary, regimes of strong integration, exceeding 100 cells may well exist at larger aperture, for f-numbers smaller than 1.5. It should be recognised that spatial integration changes neither the generic interference formula (Equation 1), nor the existence of singularities. The integrated regime, involving, say, m independent cells, obeys formally the same equation as the perfectly resolved case, on conditions of replacing the background B by the integrated background, B_+, sum of the m constituent backgrounds, and to define an integrated complex modulation, M_C – sum in the complex plane of the m independent cell modulations, whose modulus M_+ and phase φ are the resultant modulation and phase of the rewritten interferometric formula respectively. An important general result is furthermore readily obtained: M_+ drops to $1/\sqrt{m}$ with a saturating detector, but grows to $\sqrt{m}$ without saturation. From the random walk followed by the integrated modulation, it can be seen that singularities exist in integrated regimes too. In the resolved case, singularities are points of zero speckle intensity, where the phase is not defined [17, 18], thereby preventing interferometric measurements in those points. When the modulus of the integrated modulation is zero, the phase information is also lost. Singular pixels are those whose grey levels remain unchanged by phase shifting. Of note, singular pixels are discarded at the processing stage by linear sine/cosine phase filters using kernels proportional to the square of the pixel modulation – filters known to lead to the maximum-likelihood phase estimation [15, 19]. The best and more complete information that can be obtained in SI is the knowledge of the statistical properties of the background and modulation RVs in the four principal cases listed in Figure 1A. The corresponding known probability density functions allow choosing the mean intensities of the interfering waves and the aperture number optimally, so that the recordings are at their best.

Optical aspects

Within the definition given above, there are many ways to create SI arrangements. The optical viewpoint involves the examination of the different means to divide and recombine two waves, with at least one being a speckle wave (Figure 1B). Three main possibilities emerge (Figure 2):

(1) The output of the laser can be divided in order to form, on the one hand, a single illumination-observation of the object surface and, on the other hand, a reference beam, recombined in-line with the observation wave in front of the detector (Figure 2A). This recombination is said to be in-line because the angle between the object and the reference waves should be kept small enough so that the resulting fringe pattern has a carrier frequency that can be resolved by the photo-detector. The phase of the object speckle wave is changed according to the object deformation (see the next section). The reference wave can be a smooth wave, an arbitrary speckle wave or even a speckle wave arising from a macroscopically identical object for direct comparison purposes; the reference wave can be modified or not in the final state, leading to adaptive or comparative versions of the method; when the object stays at rest, small changes in the wavelength, the illumination angle, the refractive index of the medium surrounding the object, all small enough for not destroying the correlation conditions, give rise to interference phase changes related to the shape of the object; the in-line arrangement is quite close to the DH arrangement; however, in SI, no attempt is made to

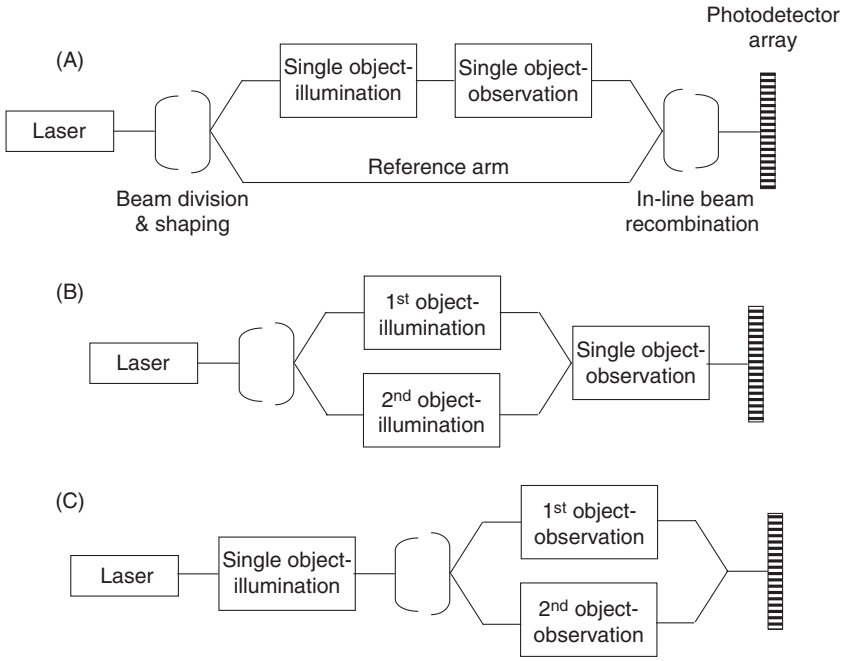

Figure 2: Diagram of the three categories of optical set-ups in SI: (A) in-line reference beam and single illumination-observation; (B) two illuminations beams; (C) two observation beams

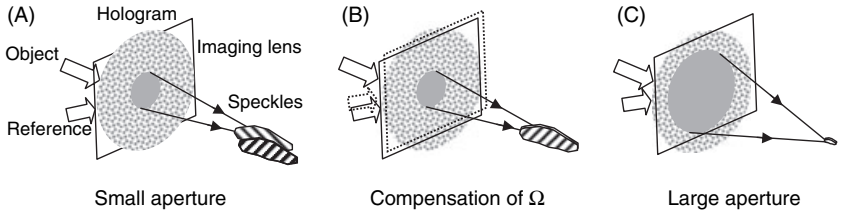

Figure 3: Fulfilling the correlation conditions in real-time HI: appropriate displacement steps of the reference beam and the hologram aim at the best superimposition of the speckle grains corresponding to the two deformation states. The subsequent increase of the lens aperture leads to the formation of smaller speckles

reconstruct, either in a numerical or analogous way, the object wave in the 3D space; only the phase of the recorded pattern in the detector plane is of concern; this important difference suffices to distinguish the SI and DH techniques unambiguously.

(2) The division of the laser beam may serve to create two illumination beams, each producing its own speckle field, and a single observation (Figure 2B). Here, both speckles are affected by the object deformation, so that the net phase increment for the new interference pattern, depicting the new state of deformation, is the difference between the two speckle phase changes. The conditions of object at rest and same modifications as before will result again in interference phase changes related to the object shape; particular cases of double illuminations include a small angular separation between the two beams, giving rise to the well-known sets of contouring methods by coherent fringe projection [20]; another interesting double illumination scheme is made of two parallel unexpanded beams interrogating two neighbouring regions of the object [21].

The separation and recombination can be performed only on the side of the observation (Figure 2C). It is still possible here to distinguish observation beams of different directions from beams only transversally shifted one with respect to the other; this latter case represents the set of well-known shearing arrangements [22]. As a result of the diffusing properties of rough surfaces, it is seen that there are much more possible arrangements in SI than in CI or grating interferometry (GI). The simple two-beam cases presented in Figure 2 can be easily extended to more complicated geometries, involving more than one reference or more than two illumination or observation beams, taken two by two, for the general purpose of information multiplexing. The diagrams presented in Figure 2 – in which the boxes 'beam division & recombination' can be any realisations of the well known types of classical interferometry, either by 'amplitude' (Michelson, Mach-Zehnder, Fizeau, Jamin, etc.) or by 'wavefront' division (Young, Fresnel bi-mirror or bi-prism, Meslin bi-lens, Smartt, etc.) – are thus nothing else

but the building blocks of innumerable set-up architectures.

Mechanical aspects

Speckle interferometry has been mainly developed for the purposes of experimental mechanics and an important part of this paper is devoted to the mechanical aspects of SI. As is well known, Equation (1) serves to code a reference state, and deterministic information is only obtained from correlated evolutions of this initial interference pattern. How does a speckle field respond to a small perturbation of the factors which led to its creation? A small perturbation may be a minute wavelength or refractive index change, a micro-displacement or deformation of the object surface, a slight modification of the illumination or observation geometry. The most thorough treatment of this question has been given in the framework of HI [4, 5, 13, 23]. Qualitatively, the answer is that the speckle field first responds locally, in a region surrounding the position vector, **r**, by a 3D displacement, Ω, without significant structural change, i.e. in maintaining the same complex amplitudes A_f and A_i, before and after the application of the perturbation:

$$A_f(\mathbf{r}+\mathbf{\Omega}) = A_i(\mathbf{r}). \tag{4}$$

This result can be readily derived from the comparison of the expressions of the diffraction integral, as e.g. the Rayleigh–Sommerfeld integral, related to the two states of object deformation. Another straightforward approach is to rely on the stationarity of the optical path difference between the two states which must be zero far all rays in the neighbourhood of the point of the surface under examination. Unfortunately, this quite simple result is heavily impaired by a series of weaknesses: there is no general relationship between Ω and the parameters of the perturbation, and, when this relationship is known in particular cases (as, e.g. wavelength change alone, or micro-deformation of the object surface limited in its description to the three displacement components and the six in-surface derivatives), it is far too much complicated to give rise to effective measurement capabilities. Moreover, the limits of validity of Equation (4), indicating the failure of the structural invariance when the amplitude of the perturbation is too large, are not clarified in any theory. This point remains essentially a matter of experimental concern. However, these drawbacks are detrimental only in defocused speckle photography, where the measured quantity is precisely Ω. In focused speckle photography, and for a perturbation involving a micro-deformation of the object surface, the situation improves already: Ω reduces to the 3D displacement vector of the surface points and the speckle grains move as if attached to the surface. In SI and HI an opposite situation must prevail: Ω must not be resolved, meaning that the correlation volume, Equation (3), must be bigger than the modulus of Ω:

$$\langle S_\mathrm{t}\rangle > |\mathbf{\Omega}|_\mathrm{t}; \quad \langle S_\mathrm{l}\rangle > |\mathbf{\Omega}|_\mathrm{l}. \tag{5}$$

Although these conditions must be fulfilled both in HI and SI, they lead to quite distinct modus operandi. In HI, and possibly in DH too, as briefly evoked at the beginning of the section, the procedure is to search in the 3D space for fringe localisation, i.e. for regions where the condition is fulfilled, and when Ω is negligibly small compared with the correlation volume, a so-called complete localisation is reached [13]. In SI, both in the cases of one or two speckle waves, the condition must be *a priori* satisfied in the recording plane. The very efficient approach followed in real-time HI, which optimises the fulfilment of Equation (5), sketched in Figure 3, is unfortunately difficult to transpose in SI. In SI, the dimensions of the correlation volume are fixed at the initial state, by choosing an appropriate aperture for the observation system, and the experiment should be restarted for testing another aperture. It should be realised that a perfect correlation between the two compared states is always elusive, because Equation (4) is basically an approximation, and because the perfect overlapping of the two states (Ω = 0), both in the pupil plane and in the observation plane cannot be granted, with the effect of modifying the final complex amplitude. Some additional comments are given in the section 'Decorrelations'. However, when the experiment shows that the initial and final states are well enough correlated and the superposition condition, Equation (5), fulfilled, the so-called correlation fringes can be obtained, generally by taking the absolute value of the difference of the two realisations $I_{\mathrm{R}f}$ and $I_{\mathrm{R}i}$ of Equation (1) leaving a distribution I_-:

$$I_- = |I_{\mathrm{R}f} - I_{\mathrm{R}i}| = 4M\left|\sin\left(\varphi + \frac{\Delta\varphi}{2}\right)\right|\left|\sin\frac{\Delta\varphi}{2}\right| \tag{6}$$

where, besides fluctuating quantities, the deterministic term $\Delta\varphi$ represents the net phase change between the two arms of the interferometer related to the perturbation applied to the interferometric arrangement. Equation (6) depicts the fringe pattern sought. For a single speckle field and in the case of micro-deformation, the general expression for the phase change is proportional to the projection of the displacement vector **L**, describing the

deformation, onto the sensitivity vector **S**, difference between the observation and illumination unit vectors $\mathbf{K}_o$ and $\mathbf{K}_e$, oriented along the bisector of the two directions:

$$\Delta\varphi = \frac{2\pi}{\lambda}(\mathbf{K}_o - \mathbf{K}_e)\cdot\mathbf{L} = \frac{2\pi}{\lambda}\mathbf{S}\cdot\mathbf{L}. \quad (7)$$

We see in the next section how $\Delta\varphi$ can be computed. According to Equation (7), there is an infinite number of ways for producing phase changes corresponding to a given object deformation. This can be simply achieved by changing the geometry of the arrangement. In experimental mechanics, the classical set-ups are the double symmetrical illumination, providing in-plane sensitivity in the direction of the plane of incidence; the in-line reference arrangement, with normal or symmetrical illumination and observation beams, giving an out-of-plane sensitivity; a shearing device placed in front of the observation lens creates two superimposed shifted images of the object surface and is sensitive to the six in-surface derivatives of the three displacement components, reducing to the slope in the shearing direction when the illumination and observation beams are orthogonal to the object surface. When the object stays at rest, the contouring of its surface can be obtained either by an in-line arrangement or by the symmetrical beam illumination, by changing the wavelength, the refractive index or the incidence of the illumination beam(s). These different possibilities are summarised in Figure 1C. From its definition, Equation (7), it is clear that the sensitivity vector is generally not constant over the object surface. Only parallel beam illumination and telecentric observation can guarantee the constancy of the sensitivity vector, which is only possible for small objects. For spherical illumination wave and observation system ruled by central projection, the sensitivity is never purely associated with a single component over the whole surface. When small compared with the main component of the deformation, the unwanted components can however often be neglected by selecting a sensitivity vector as orthogonal as possible to these components. Nonetheless, the actual trends in experimental mechanics are to create more and more precise analytical or numerical models. This is a strong incentive to try to solve the general three-component (3C)–3D problem, i.e. to determine the three components of the displacement for 3D, arbitrarily shaped objects. Several sensitivity vectors are needed – at least three and more when the absolute fringe order cannot be assessed [24].

Two categories of solutions exist, endowed with their own advantages and drawbacks:

1 an arrangement with multiple illuminations only [25];
2 an arrangement with multiple illumination and in-line reference [26].

Both categories lend themselves to shape measurement of the object and sensitivity vector determination. The multiple illumination scheme, with a single observation and without the burden of an in-line reference is simple to realise and adjust, especially by means of optical fibres. By switching on two by two the illumination beams, sensitivity vectors equal to the difference of the two unit vectors of the concerned illuminations are created. The resultant linear system from Equation (7) is inverted to recover the three displacement components. The scheme including an in-line reference is a bit more complicated, but smooth reference wave interferometers generally give less noisy interferometric signals and make a better use of the available laser power. Here again, the necessary equations are obtained by switching on one by one the different illumination beams, while always keeping the same reference. Both schemes have their own predominant sensitivities and care should be exercised to produce well-conditioned systems [27]. It is also possible to create synthetic sensitivity vectors by computing linear combinations of Equation (7). Multiplexing of the recordings is a serious problem. In the hypothesis of a phase computation by a three-image phase-shifting algorithm, the acquisition of at least 24 interferograms is needed to solve the 3C-3D problem. This number grows to 50 for a five-image algorithm and a fourth redundant equation. Furthermore, not only specific to SI, but also mandatory, are the geometrical and radiometric calibrations of the observation system. The mapping between the pixel coordinates and the 3D surface coordinates must be known. As a start, the simplest procedure, based on the pinhole camera model requires the determination of no less than nine parameters. The linearity and the uniformity of the photo-electric response of each pixel must be verified and corrected if necessary. The solution of the 3C–3D problem is not at all simple. There are very few examples of a complete and careful application of the above procedures [25, 26]. A sound analysis of what should be measured should thus accompany the design of any SI experiment.

Processing aspects

A last possible categorisation of SI techniques is linked to the principal processing routines (Figure 1D). This is perhaps the domain still most open to new ideas; the successive proceedings of the 'Fringe' Conferences series give the principal milestones [28]. Here, the main distinction appears to be between the static and dynamic regimes of deformation. Exposure types – continuous, time average, pulsed, stroboscopic – also play a discriminating role. In static measurements, the most used and worth recommending technique is phase-shifting [29]. The phase is computed by an analytical expression involving linear combinations of the grey levels I_{Ri} of n recordings, each obtained for a known, externally applied, additional phase shift:

$$\varphi = \tan^{-1}\left[\frac{\sum_{i=1}^{n} \alpha_i I_{Ri}}{\sum_{i=1}^{n} \beta_i I_{Ri}}\right]; \quad \varphi \in [0, 2\pi] \tag{8}$$

where α_i and β_i are known coefficients depending on the retained algorithm. Applied two times, for each of the two object states under comparison, Equation (8) gives two digital random and correlated phase maps, whose difference is the deterministic phase map of Equation (7). Figure 4 illustrates the phase-shifting procedure in SI (an in-line reference arrangement here) for a three-image algorithm with phase-shifts of 120°. Except the specimen loading, the time taken by the full procedure is mainly dependent on the system acquisition rate and the time constant of the phase-shifting device. For the three-image algorithm, a standard figure is of the order of a quarter of a second. A full library of algorithms is available and phase-shifting techniques have achieved very high performances. Phase maps are notably less noisy than correlation fringes, because phase-shifting is also a powerful averaging process. The only inconvenience lies in the necessity to ensure an interferometric stability during the time taken to acquire the n phase-shifted recordings. Phase-shifting techniques can be applied to some extent to dynamic situations, assuming that the total phase shift between two consecutive recordings is the sum of an external shift, say $\pi/2$, and of the unknown

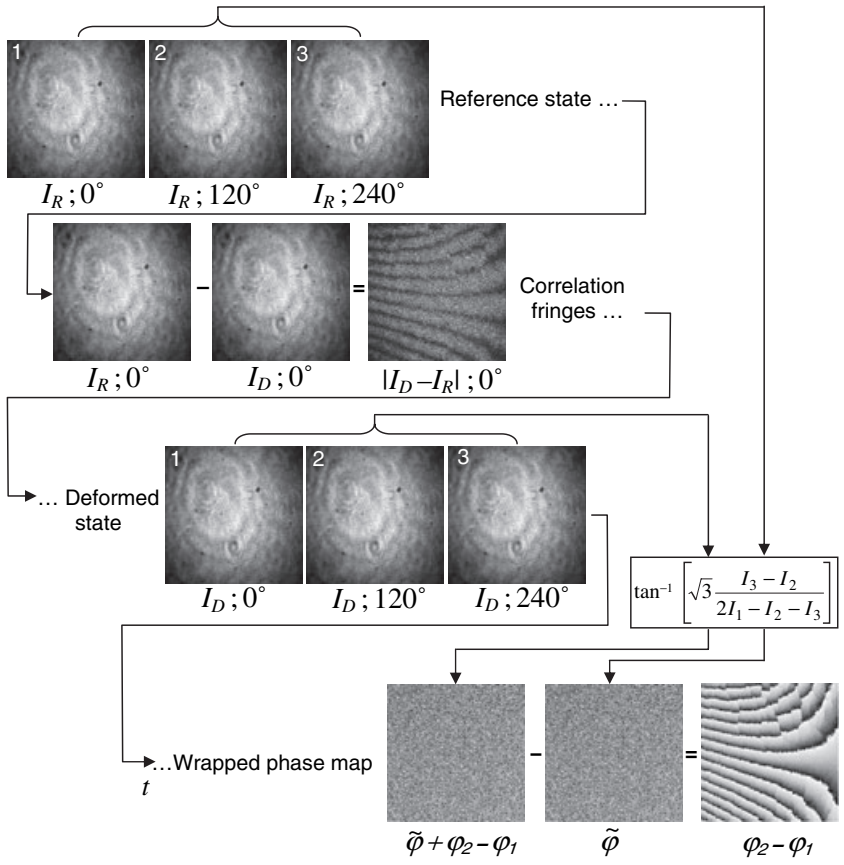

Figure 4: Phase-shifting processing of SI fringe patterns, illustrated by the three-image algorithm. Three fringe pattern, corresponding to external phase shifts of 0°, 120° and 240°, are acquired in the reference and deformed states; in the mean time, correlation fringes are produced by a real-time absolute subtraction between the reference and deformed fringe patterns in order to monitor the deformation; finally, the phase maps of the two states are computed by the $\tan^{-1}$ formula, leading, by subtraction, the phase map related to the object deformation and obeying the sensitivity formula

object phase increment itself, considered as constant over the four to five frames needed, and proportional to the slope of the object phase at this moment [30]. Four- or five-image algorithms account for the additional unknown. Dynamic phase-shifting is limited to situations where the ratio (frame rate/phase change rate) is high. For broader dynamic situations, several standard solutions exist, based either on the spatial processing of 2D interferograms acquired in a single frame mode, or on the temporal processing of the 1D pixel signals of sequence of frames. In both cases, the introduction of an external carrier frequency, spatial or temporal, is advantageous for removing the sign ambiguity and for a more accurate phase extraction. The best known and widely used methods rely either on definite transforms, as Fourier, Morlet wavelet, modified 2D Hilbert transforms [31–33], or on correlation techniques [34, 35]. A new trend is to reshape the interferometric signal into a sinusoidal form amenable to more standard processing, using signal-dependent transformation [36]. Vibration analysis is an important sub-domain of dynamic regimes and has received as much attention in SI as in HI [37]. Procedures are available to obtain simultaneously the amplitude and phase of the mechanical vibrations. It should be acknowledged that DH completely escapes the dynamic regime difficulty, because amplitude and phase of the object are numerically reconstructed from the recording of a single interferogram. [0–2π] or wrapped phase maps are efficiently filtered by linear filters applied to the sine and cosine of the phase images. The last step of the processing, phase unwrapping, not specific to SI, formed the subject of many studies; many operational algorithms are available, just open to improvements [38]. From the processing point of view, and contemplating the high quality reached by the phase maps, SI now enjoys a good status – certainly equivalent to the other whole-field methods – and much better than in the past, when

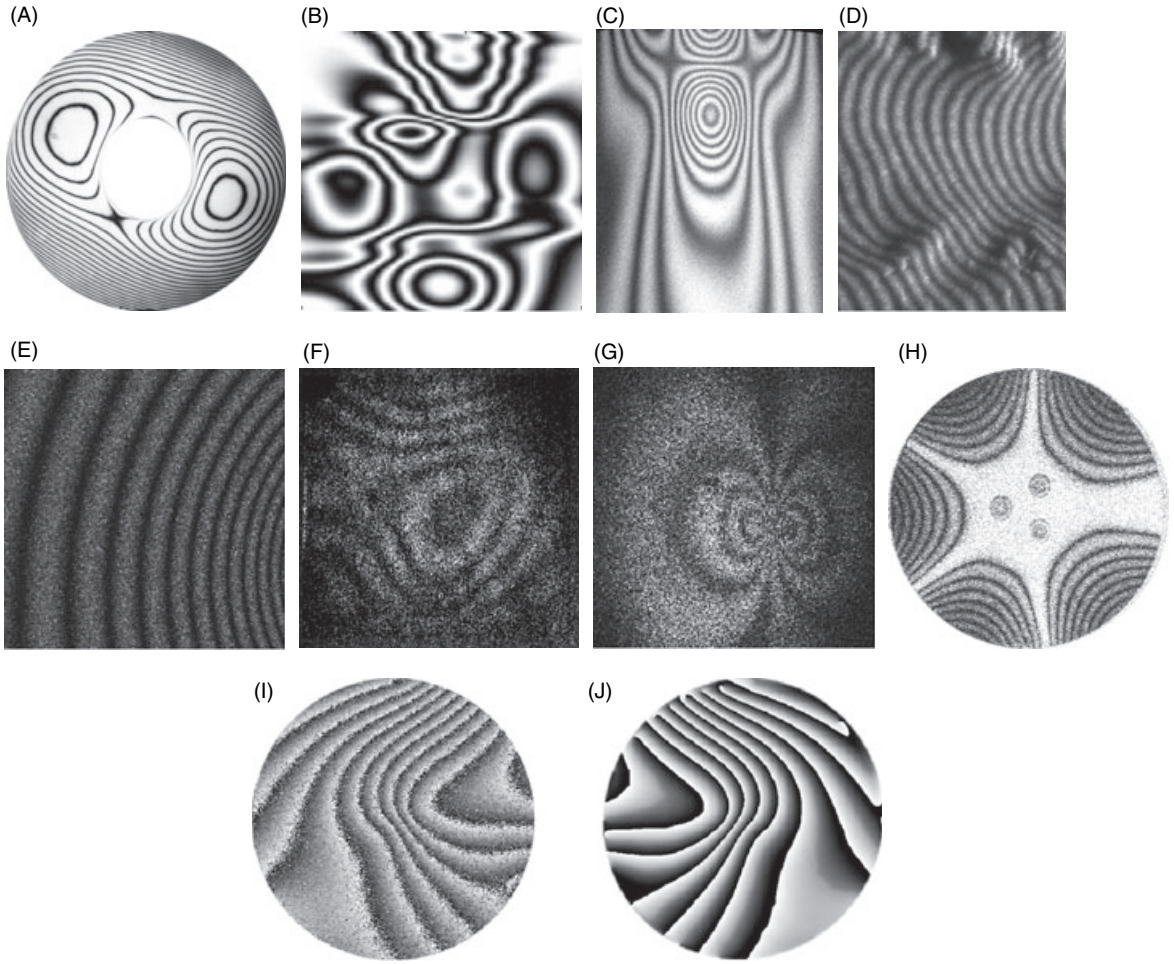

Figure 5: Examples of fringe patterns highlighting the differences between 'classical' (A–D) and SI fringes (E–J): (A) classical Fizeau fringes of a computer hard disc; (B) MATLAB 'peaks' function depicted as a classical fringe pattern; (C) HI fringes of a cylinder locally heated; (D) contouring using coherent fringe projection on a cast of pathological scar; (E) simulated ideal SI correlation fringes; (F) out-of-plane fringes of a 2.8×4 m^2 plaster wall; (G) shearing SI fringes of the same wall locally heated; (H) out-of-plane Bessel-type fringes of a disc vibrating at a resonance frequency of 1.9 kHz; (I) SI phase map: rough result of a five-image phase-shifting algorithm; (J) the same map after linear sine–cosine filtering

the then heavily speckled aspects of the interferograms raised doubts about the value of the recorded information. This assessment is backed up by Figure 5, which shows a series of interferograms obtained in classical or holographic interferometry, of high quality, whereas SI correlation fringes exhibit their characteristic grainy aspects. Even so, the final quantitative SI result represented by the phase maps, obtained by the processing procedures mentioned above, is fully satisfactory.

Decorrelations

The two compared interferograms associated with the reference and deformed states of the specimen differ more than only by the deterministic phase factor of Equation (7). Because of the object displacement field, speckle grains do not superimpose exactly in the image plane. They are not even exactly the same, in particular because the speckle wavefront is displaced and deformed in the plane of the pupil. The actual final phase maps are thus fundamentally the result of a much more intricate series of phenomena than those described above. While in principle completely deterministic, these phenomena cannot be tackled by analytical relationships. The reason is that, because of the form of the diffraction integrals, the derivations would necessitate a perfect knowledge of the surface micro-roughness and its evolution. The only practical approach – still quite involved itself – is statistical [15, 16, 19, 39]. A brief summary of the findings presented in the later reference is given below.

Eight separate cases should be treated, made of the two decorrelation sources – pupil and image plane, the two types of interference – two speckles or one speckle and one smooth wave, and the two spatial integration regimes – resolved or not resolved. Let us define the phase error as the difference between the phase of Equation (7) and the actual phase involving the decorrelation effects. The probability density function of the phase error is formally the same for seven cases. The only exception is for the case, pupil plane decorrelation, two speckles, unresolved speckles, which is without analytical expression. However, the behaviour of the standard deviation of the phase error in this case can be estimated as $\sqrt{2}$ times greater than the other cases. The probability densities are not repeated here, because they are not easily interpretable. On the other hand, Figure 6 reproduces the evolution of the standard deviation of the phase error, σ_φ, as a function of the decorrelation parameter Δ, ratio of the common to the total area between the displaced patterns, varying between 0 and 1. The rule for the composition of the pupil and image decorrelations reads:

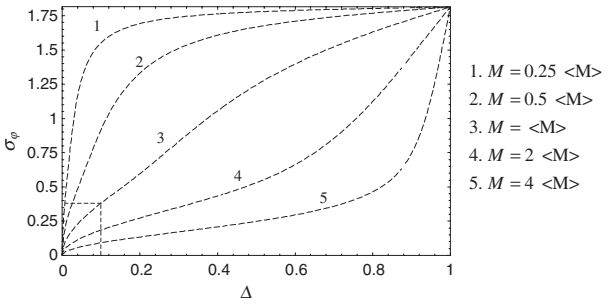

Figure 6: Standard deviation σ_φ of the phase error associated to pupil and image plane decorrelation effects as a function of the normalised decorrelation parameter Δ, for different values of the modulation M [39]

$$1 - \Delta_t = (1 - \Delta_p)(1 - \Delta_i) \quad (9)$$

with Δ_t the total decorrelation parameter and the subscripts 'p' and 'i' designating the pupil and image plane decorrelation parameters respectively. The diagram confirms the primary role played by the modulation M, cf. Equations (2) and (6), a strong modulation meaning much smaller errors. The standard deviation of the phase error is rapidly quite high, 0.1 of the decorrelation parameter producing already a σ_φ of 0.38 rad at the mean modulation. While phase-shifting in itself is usually easily accurate to 0.06 rad, the phase error in SI is rather five times less accurate or even worse. It can also be seen that near the total decorrelation, the standard deviation, as expected, tends towards $\pi/\sqrt{3}$, the standard deviation of a uniform distribution over $[-\pi, \pi]$.

Pupil and image plane decorrelations should be avoided as much as possible. Image plane decorrelations can be efficiently combated by physical or numerical re-superimposition of the speckle fields. A general measure for decreasing pupil plane decorrelation effects is to work with large apertures. In both cases, fractioning the total deformation into n loading steps of magnitude $1/n$, as well as preventing rigid-body motions of the specimen, is also quite rewarding. Linear sine–cosine phase map filtering using kernel proportional to the square of the modulation is an additional effective improvement.

Strengths

As an interferometric method, the sensitivity of SI is basically of 2π per λ optical path change. Taking in account the existing fringe interpolation techniques, the displacement measurement range and the displacement resolution are thus of the order of 10 nm to 10 μm and 10 nm per loading step respectively. These characteristics are extraordinarily well adapted to the

general requirements of experimental mechanics, a great number of mechanical phenomena occurring at this scale. As an imaging technique based on photo-electric arrays, millions of points can be interrogated simultaneously, each pixel acting *a priori* as an independent detector. In a sound designed experiment, the lens aperture and magnification, the pixel dimension and the wavelength are such that the pixel has just the transversal dimension of the correlation volume (Equation 3). Consequently, the effective spatial resolution, before linear filtering, is the spatial resolution of the recording medium. The overall performances of SI in spatial, temporal and measurement resolutions are thus exceptionally high, only challenged by classical HI. But classical HI suffers a strong recession stage simply because high spatial resolution media have progressively ceased to be commercially available. Tied to the intrinsic properties of SI, the photo-electric technology introduces many advantages: real-time visualisation, high radiometric sensitivity, simplicity, robustness, no consumables and low cost. Its connection with computer and digital image processing is considerably developed and the future in these domains can only be still brighter. With its innumerable arrangements and not requiring specific surface preparations, SI counts an impressive set of variants, showing extreme flexibility and the possibility to choose multiple displacement sensitivities, both in the nature and the magnitude of the components. None of the other whole-field interferometric techniques – Cl, GI, HI, DH – exhibit such a high degree of adaptability to many experimental situations.

Weaknesses

Even if very high spatial resolution recording media are avoided, SI is nonetheless an interferometric technique and, except for the object deformation, no perturbation likely to change the optical path lengths between the two arms of the interferometer by more than a fraction of the wavelength during the exposure time should intervene. This is an obvious requirement when the aim is to measure displacements with a resolution in the nanometric range. A more serious and fundamental problem lies in the fulfilment of the correlation conditions. As indicated previously, the problem is theoretically hard, not fully treated. The solution still rests mainly on tedious experimental trial and error procedures. The compensation of speckle displacements in the pupil and in the image plane is not easy in SI as in HI. The absence of high spatial resolution medium forces us to use lens apertures moderately open and explains the residual grainy aspects of the interferograms. If σ_φ denotes the standard deviation of the phase error currently found in the usual practice of CI, GI, HI, DH and SI, the following ranking can be established [15, 40]:

$$\sigma_\varphi(\mathrm{CI}) \approx 0.1^\circ < \sigma_\varphi(\mathrm{GI}) \approx 0.4^\circ < \sigma_\varphi(\mathrm{HI}) \approx 1^\circ < \sigma_\varphi(\mathrm{DH}) \approx \sigma_\varphi(\mathrm{IS}) \approx 10^\circ \quad (10)$$

A series of measures, briefly evoked above, aiming at a better fulfilment of the correlation conditions and at reducing the effects of the perturbations have been proposed and proved effective [11, 15, 41]. Yet, these measures, sometimes difficult to implement, are still to be improved. As a final weak point, powerful continuous wave (CW) or pulsed laser sources for large objects in difficult environments are, for the time being, expensive.

Opportunities

The list of mechanical applications of SI is impressively long [6, 42]. A full paper would not suffice to present, even shortly, the most significant of them. The future is essentially dependent on the needs and expectations of experimental mechanics. Now, there are many signs that the demand is strongly up. All major branches of experimental mechanics – material properties, structural analysis, non-destructive testing – are facing challenges of unprecedented complexity. As exemplified by civil or aeronautical engineering, the trends are towards ever more streamlined constructions, having to bear record loadings, while under increasingly severe environmental constraints and security levels. Modelling tasks need to be more and more accurate and computer simulations must be checked carefully. SI can certainly take advantage of this favourable orientation of experimental mechanics. Structural and material property identification, modelling assessment, residual stress, rheology, damage and ageing are in particular the sub-fields where SI looks likely to become a standard tool. The next chance of SI is in its very constitution: it is naturally boosted by the continuous progress of electronic imaging and digital image acquisition and processing. SI remains open to significant improvements, in particular in the sense of becoming a genuine adaptive method, efficient against external perturbations, thanks to the rapid development of phase modulators. Continuous progresses in speed, independence from the operator, reliability, made on the side of the processing of the acquired patterns are very encouraging. Even if it appears as a brute-force

solution, the strong increase of the volume of recorded data allowed by present-day computers, when supplemented by clever data reduction methods, considerably extends the applicability of SI. As simple yet pertinent numerical models for the mathematical generation of speckle fields are available [43], the same computing power may be used to simulate SI experiments, for testing or benchmarking processing programmes or checking the efficiency of particular configurations, thereby contributing to the success of the method. Finally, by shifting to low coherence sources, SI has the prospect to become a whole-field optical coherence tomography (OCT) method, allowing the exploration of an important and completely new field: performing deformation measurements in the bulk of 3D diffusing media [44, 45].

Threats

As an established method, SI does not appear to be spoilt by appalling shortcomings. Perhaps the greatest peril for SI (but not for photomechanics!) would be the appearance of a new very efficient high spatial resolution photosensitive material, liable to be easily processed *in situ*, something similar to the photorefractive crystals, but with much better radiometric sensitivity and more manageable erasure. In this case, HI techniques would probably recover a prominent place. Another possible obstacle would be that the photomechanics community massively prefers the rival image correlation techniques, under the questionable pretexts of simplicity. This would be a worrying choice. In fact, without denying the qualities of image correlation techniques, it is probably wrong to bring the two types of methods into conflict. Real-time operation, spatial, temporal and measurement resolutions on the side of SI, simplicity and apparent robustness for image correlation are some of the features which clearly separate the two types of method. The last danger lies in the near non-existence of a structured and coordinated teaching of SI: unfortunately, very few engineering curricula integrate it into their programmes.

Conclusion

It is hoped that these few thoughts about SI will reinforce the practitioners' faith in the soundness of their choice and encourage newcomers to acquire the scientific background and the optical equipment needed for sound and successful operations of the method.

ACKNOWLEDGEMENTS

This study was mainly supported by Swiss National Science Foundation grants.

REFERENCES

1. Leendertz, J. A. (1970) Interferometric displacement measurement on scattering surfaces utilizing speckle effect. *J. Phys. E: Sci. Instrum.* **3**, 214–218.
2. Butters, J. N. and Leendertz, J. A. (1971) Speckle pattern and holographic techniques in engineering metrology. *Opt. Laser Technol.*, **3**, 26–30.
3. Dainty, J. C. (Ed.) (1975) *Laser Speckle and Related Phenomena*. Springer Verlag, Berlin.
4. Jones, R. and Wykes, C. (1989) *Holographic and Speckle Interferometry*. Cambridge University Press, Cambridge.
5. Dändliker, R. and Jacquot, P. (1992) *Holographic Interferometry and Speckle Techniques. Optical Sensors*. VCH Verlagsgesellschaft, Weinheim, 589–628.
6. Meinlschmidt, P., Hinsch, K. D. and Sirohi, R. S. (Eds) (1996) *Selected Papers on Electronic Speckle Pattern Interferometry: Principles and Practice*. SPIE Milestone Series, SPIE Optical Engineering Press, Bellingham, WA, Vol. MS 132.
7. Jacquot, P., and Fournier, J.-M. (Eds) (2000) *Interferometry in Speckle Light: Theory and Applications*. Springer, Berlin.
8. Slangen, P., and Cerruti, C. (Eds) (2006) *Speckle06*. Proc. of SPIE, Nîmes, France, Vol. 6341.
9. Stetson, K. A. (2001) *Roads not Taken in Holographic Interferometry. Fringe 2001*. Elsevier, Paris, 581–586.
10. Trolinger, J., Markov, V. and Khizhnyak, A., (2005) Applications, challenges, and approaches for electronic, digital holography. *Proc. of SPIE* **6252**, 625218-1-11.
11. Jacquot, P. (2005) Speckle interferometry: refining the methods for taming disorder. *Proc. of SPIE* **6252**, 62521S-1-12.
12. Stetson, K. A. and Powell, R. L. (1965) Interferometric hologram evaluation and real-time vibration analysis of diffuse objects. *J. Opt. Soc. Am.*, **54**, 1964–1965.
13. Schumann, W. and Dubas, M. (1979) *Holographic Interferometry*. Springer Verlag, Berlin.
14. Goodman, J.W. (1975) *Statistical Properties of Laser Speckle Patterns. Laser Speckle and Related Phenomena*. Springer Verlag, Berlin, 9–75.
15. Lehmann, M. (1998) *Statistical Theory of Two-wave Speckle Interferometry and its Application to the Optimization of Deformation Measurements*. EPFL thesis, Swiss Federal Insitute of Technology, Lausanne, no. 1797.
16. Lehmann, M. (1996) Phase-shifting speckle interferometry with unresolved speckle: a theoretical investigation. *Opt. Comm.* **128**, 325–340.
17. Baranova, N. B., and Zel'dovich, B. Y. (1981) Dislocations of the wave-front surface and zeros of the amplitude. *Sov. Phys. JETP* **53**, 925–929.
18. Freund, I. (1994) Optical vortices in Gaussian random wave fields: statistical probability densities. *J. Opt. Soc. Am.* **11**, 1644–1652.

19. Huntley, J. M. (1995) Random phase measurement error in digital speckle pattern interferometry. *Proc. of SPIE*, **2544**, 246–257.
20. Liu, H., Lu, G., Wu, S., Yin, S. and Yu, F. T. S. (1999) Speckle-induced phase error in laser-based phase-shifting projected fringe profilometry. *J. Opt. Soc. Am. A* **16**, 1484–1495.
21. Kadono, H., Bitoh, Y. and Toyooka, S. (2001) Statistical interferometry based on a fully developed speckle field: an experimental demonstration with noise analysis. *J. Opt. Soc. Am. A* **18**, 1267–1274.
22. Steinchen, W. and Yang, L. (2003) *Digital Shearography*. SPIE Press, Bellingham, WA.
23. Stetson, K. A. (1976) Problem of defocusing in speckle photography, its connection to hologram interferometry and its solution. *J. Opt. Soc. Am.* **66**, 1267–1670.
24. Siebert, Th., Splitthof, K. and Ettemeyer, A. (2004) A practical approach to the problem of the absolute phase in speckle interferometry. *J. Hologr. Speckle* **1**, 32–38.
25. Goudemand, N. (2005) *3D-3C Speckle Interferometry: Optical Device for Measuring Complex Structures*. ETHZ thesis, Swiss Federal Institute of Technology, Zürich, no. 15961.
26. Gautier, B. (2005) *Etudes et réalisation d'un interféromètre de speckle à mesure de forme intégrée*. Thèse Ecole des Mines de Paris, Paris.
27. Osten, W. (1985) Some considerations on the statistical error analysis in holographic interferometry with application to an optimized interferometer. *Opt. Acta*, **32**, 827–838.
28. Jüptner, W. and Osten, W. (Eds) (1989) (1993) (1997) (2001) (2005) *Proceedings of the ''Fringe'' Conferences Series*. Akademie Verlag, Berlin (89-93-97), Elsevier, Paris (01), Springer, Berlin (05).
29. Creath, K. (1988) *Phase-Measurement Interferometry Techniques*, Progress in Optics XXVI. Elsevier Science Publishers B.V., Amsterdam, 349–393.
30. Colonna de Lega, X. and Jacquot, P. (1996) Deformation measurement with object-induced dynamic phase-shifting. *Appl. Opt.* **35**, 5115–5121.
31. Takeda, M., Ina, H. and Kobayashi S. (1982) Fourier-transform method of fringe-pattern analysis for computer-based topography and interferometry. *J. Opt. Soc. Am.* **72**, 156–160.
32. Colonna de Lega, X. (1997) *Processing of Non-stationary Interference Patterns: Adapted Phase-shifting Algorithms and Wavelet Analysis. Application to Dynamic Deformation Measurements by Holographic and Speckle Interferometry*. EPFL thesis, Swiss Federal Institute of Technology, Lausanne, no. 1666.
33. Larkin, K. G. (2001) Natural demodulation of two-dimensional fringe patterns. I. General background of the spiral phase quadrature transform & II. Stationary phase analysis of the spiral phase quadrature transform. *J. Opt. Soc. Am. A* **18**, 1862–1881.
34. Servin, M., Marroquin, J. L. and Quiroga, J. A. (2004) Regularized quadrature and phase tracking from a single closed-fringe interferogram. *Opt. Im. Sci. Vis.* **21**, 411–419.
35. Robin, E., Valle, V. and Brémand, F. (2005) Phase demodulation method from a single fringe pattern based on correlation technique with a polynomial form. *Appl. Opt.*, **44**, 7261–7269.
36. Equis, S., Baldi, A. and Jacquot, P. (2007) Phase Extraction in Dynamic Speckle Interferometry by Empirical Mode Decomposition. *CDR Proc ICEM13 Conf*, Alexandroupolis, Greece.
37. Doval, A. F. (2000) A systematic approach to TV holography. *Meas. Sci. Tech.* **11**, R1–R36.
38. Ghiglia, D. C. and Pritt, M. D. (1998) *Two-dimensional Phase Unwrapping: Theory, Algorithms, and Software*. Wiley, New York.
39. Lehmann, M. (1997) Decorrelation-induced phase errors in phase-shifting speckle interferometry. *Appl. Opt.* **36**, 3657–3667.
40. Thalmann, R., and Dändliker R. (1986) Statistical properties of interference phase detection in speckle fields applied to holographic interferometry. *J. Opt. Soc. Am. A.* **3**, 972–981.
41. Svanbro, A. and Sjödahl M. (2006) Complex amplitude correlation for compensation of large in-plane motion in digital speckle pattern interferometry. *Appl. Opt.* **45**, 8641–8647.
42. Jacquot, P., Fournier, J.-M., Gastinger, K., Løkberg, O. J., Winther, S., Slangen, P. and Cerruti, C. Eds. (2000, 2003, 2006) *Proceedings of the ''Speckle'' Conferences Series*. Lausanne, Trondheim, Nîmes.
43. Equis, S. and Jacquot, P. (2006) Simulation of speckle complex amplitude: advocating the linear model. *Proc. SPIE* **6341**, 634138-1–6.
44. Gülker, G., Hinsch, K. D. and Kraft, A. (2001) Deformation monitoring on ancient terracotta warriors by microscopic TV-holography. *Opt. Lasers Eng.* **36**, 501–512.
45. Ruiz, P. D., Huntley, J. M. and Wildman, R. D. (2005) Depth-resolved whole-field displacement measurements by wavelength scanning electronic speckle pattern interferometry. *Appl. Opt.* **44**, 3945–3953.

